Morphology and Rheological Behavior of Maltene–polymer Blends. I. Effect of Partial Hydrogenation of Poly(styrene-*block*-butadiene-*block*–styrene-*block*)-Type Copolymers

Paola González-Aguirre,[1] Luís Medina-Torres,[1] Cornelius Schrauwen,[2] Christian Fonteix,[2] Fernand Pla,[2] Rafael Herrera-Nájera[1]

[1]*Facultad de Química, Departamento de Ingeniería Química, Universidad Nacional Autónoma de México, Mexico DF 04510, Mexico*
[2]*Laboratoire des Sciences du Génie Chimique, Nancy-Université, Centre National de la Recherche Scientifique, 1 Rue Grandville, BP 20451 F-54001 Nancy, France*

Received 24 May 2007; accepted 15 November 2007
DOI 10.1002/app.28845
Published online in 4 February 2009 Wiley InterScience (www.interscience.wiley.com).

ABSTRACT: Because of the importance of the maltene–polymer interaction for the better performance of polymer-modified asphalts, this article reports the effects of the molecular characteristics of two commercial poly(styrene-*block*-butadiene-*block*-styrene-*block*) (SBS) polymers and their partially hydrogenated derivatives [poly{styrene-*block*[(butadiene)$_{1-x}$–(ethylene-*co*-butylene)$_x$]-*block*-styrene-*block*} (SBEBS)] on the morphology and rheological behavior of maltene–polymer blends (MPBs) with polymer concentrations of 3 and 10% (w/w). Each SBEBS and its parent SBS had the same molecular weight and polystyrene block size, but they differed from each other in the composition of the elastomeric block, which exhibited the semicrystalline characteristics of SBEBS. Maltenes were obtained from Ac-20 asphalt (Pemex, Salamanca, Mexico), and the blends were prepared by a hot-mixing procedure. Fluorescence microscopy images indicated that all the blends were heterogeneous, with polymer-rich and maltene-rich phases. The rheological behavior of the blends was determined from oscillatory shear flow data. An analysis of the storage modulus, loss modulus, complex modulus, and phase angle as a function of the oscillatory frequency at various temperatures allowed us to conclude that the maltenes behaved as pseudohomogeneous viscoelastic materials that could dissipate stress without presenting structural changes; moreover, all the MPBs were more viscoelastic than the neat maltenes, and this depended on both the characteristics and amount of the polymer. The MPBs prepared with SBEBS were more viscoelastic and possessed higher elasticity than those prepared with SBS. © 2009 Wiley Periodicals, Inc. J Appl Polym Sci 112: 1330–1344, 2009

Key words: blends; block copolymers; microstructure; morphology; rheology

INTRODUCTION

Systematic studies on composite materials have allowed the development of materials with interesting properties at relatively low cost. Examples of such materials are polymer-modified asphalts (PMAs).[1] Asphalt modification is driven by the fact that neat asphalt is a thermoplastic material with relatively poor thermomechanical properties because it is fragile at low temperatures ($<-10°C$) and soft at high temperatures ($>60°C$). The thermomechanical properties of asphalt are essentially dependent on its composition. In general, asphalt is considered a mixture of a large number of hydrocarbon species with minor amounts of functional groups such as oxygen, nitrogen, sulfur, vanadium, and nickel; hence, it is difficult to establish the precise composition of such a complex organic mixture.[2] Nevertheless, these hydrocarbons are subdivided into two broad groups, namely, asphaltenes and maltenes; the asphaltenes are highly polar aromatic hydrocarbons and have the highest molecular weight, whereas maltenes consist of low-molecular-weight saturates, aromatics, and resins.[1,3] From a rheological perspective, asphalt also constitutes a highly complex material, varying from a viscous character to an elastic character according to the loading time and temperature.[4] At low temperatures or high loading frequencies, conventional asphalt behaves as a glasslike, elastic solid, whereas at high temperatures or low loading frequencies, it behaves as a viscous fluid. Asphalt presents a time–temperature dependence involving applied stresses and resultant strains, exhibiting a response with both elastic and viscous components.[5]

Correspondence to: R. Herrera-Nájera (rherrern@servidor.unam.mx).

Contract grant sponsor: Consejo Nacional de Ciencia y Tecnología; contract grant number: PCP #09/05.

Contract grant sponsors: Société francaise d'exportation des ressources éducatives (SFERE) (France), Dynasol Elastómeros (México), Universidad Nacional Autónoma de México; contract grant number: DGAPA-IN103707.

Journal of Applied Polymer Science, Vol. 112, 1330–1344 (2009)

According to the emulsion model,[3] neat asphalt can be described as micelles of resin-stabilized asphaltenes dispersed in surrounding maltenes. At low temperatures (<10°C), neat asphalt exhibits fragile mechanical behavior because both maltenes and asphaltenes are close to their glassy region (−25°C); in contrast, at higher temperatures (>60°C), asphalt behaves as a viscoelastic fluid because the maltenes are in a liquid state and the asphaltene particles have important Brownian movements.[6]

On the other hand, PMAs are composite materials that exhibit less temperature susceptibility and higher resistance to permanent deformation than conventional asphalts.[7,8] Since the early 1970s, several types of polymers have been used to modify asphalt,[8,9] and in some cases, chemical modification has been involved.[10] Examples of polymers that have been used as asphalt modifiers include natural rubber,[11] poly(ethylene-*co*-vinyl acetate),[5,12] atactic polypropylene,[13] high-density polyethylene,[8,14] poly (styrene-*block*-butadiene-*block*),[7,15] poly(styrene-*block*-butadiene-*block*-styrene-*block*) (SBS),[7,16] poly(styrene-*block*-ethylene-*block*-butylene-*block*-styrene-*block*) (SEBS),[17] and recently poly{styrene-*block* [(butadiene)$_{1-x}$–(ethylene-*co*-butylene)$_x$]-*block*-styrene-*block*} (SBEBS) copolymers.[18] However, the type of polymer most commonly used for asphalt modification is SBS, particularly for road paving. In general, modifiers should be compatible with the asphalt and cost-effective and should resist degradation during mixing and storage and at application temperatures.[5,8,10] The effectiveness of a modification depends on the characteristics of the asphalt, the type and relative amount of the polymer, and the kind of process used to prepare the PMA. The SBSs are fine asphalt modifiers because their chemical composition, structure, and polarity make them suitable for blending with a fairly large number of asphalts without serious problems of solubility and phase segregation. The structure of neat SBS consists of styrene–butadiene–styrene triblock chains, which undergo microphase segregation leading to a two-phase morphology of spherical polystyrene domains within a matrix of polybutadiene.[7,19] The strength and flexibility of SBS result from the physical crosslinking of the two phases into a three-dimensional network in which the polystyrene end blocks impart strength, whereas the polybutadiene midblocks give SBS its special flexibility. However, polybutadiene unsaturated bonds uphold polymer degradation when they are exposed to highly oxidizing agents and mechanical stresses, and this explains the growing demand for polymers with asphalt-modifying capabilities similar to those of SBS but with higher thermomechanical resistance.[16,17] From this perspective, SEBS and SBEBS seem to be interesting options. However, there are controversial results regarding the benefits of using SBEBS for asphalt modification.[16–18] Some reports indicate that saturation of the polybutadiene double bonds makes SBEBS more rigid than SBS; therefore, SBEBS helps to improve rutting resistance but is less effective in enhancing the fatigue properties of the PMA at intermediate temperatures.[16,17] Also, SBEBS is considerably less polar than SBS and so is less compatible with asphalt.

Most PMAs are produced by high-temperature mechanical dispersion of the polymer in molten asphalt (~180°C, 2–4 h). During such processes, SBS and maltenes interact, resulting in a maltene swelling of the polybutadiene block, whereas the polystyrene blocks show practically no swelling, thus creating the so-called polymer-rich phase.[17,19,20] The volume fraction of the polymer-rich phase could reach up to 9 times its initial volume,[9,20,21] and for that reason, the addition of relatively small amounts of the polymer (~3 wt %) significantly changes the rheological properties of the asphalt.[1,4,10] The polymer-rich phase is considered a three-dimensional thermoplastic network composed of nodules of polystyrene blocks interconnected through the maltene-swollen polybutadiene blocks,[1,7,9,22] being similar to that of neat SBS. Thus, PMAs with SBS consist of a polymer-rich phase and an asphaltene-rich phase both embedded in maltenes, and the morphology and rheological behavior of the PMAs are determined by the relative amounts and characteristics of such phases. The phase separation confirms the incompatibility that exists between some of the components of the asphalt and those of the polymer. However, it is thought that the viscoelastic character of the maltene-swollen SBS is conferred to PMAs by an appropriate balance of compatibility and thermodynamic immiscibility of the asphalt and polymer.[14,17,22] The importance of the rheological behavior of the polymer-rich phase in favor of the PMA performance has also been demonstrated with the Palierne emulsion model.[4,15,23,24] According to the emulsion model, a given PMA is composed of an asphalt matrix and a polymer-rich phase, the latter being a concentrated solution of maltenes and polymer, and the rheological behavior of the PMA is modeled by consideration of the contribution of the complex modulus (G^*) of these two parts as well as their hydrodynamic interactions, the particle size distribution, and interfacial tension.[24–27] The asphalt matrix and the polymer-rich phase are obtained by the subjection of the PMA to a static hot-storage procedure[28] (160°C for 7 days), and these two parts are characterized by rheological analysis to obtain the asphalt matrix and the polymer-rich phase moduli, which are then used to predict the PMA's rheological behavior. All these efforts confirm the importance of the maltene–polymer interaction, but

unexpectedly, there have been few studies in which the maltene–polymer interaction has been explicitly explored.[22] Therefore, it was considered opportune to carry out a systematic study on maltene–SBS and maltene–SBEBS blends with four different polymers: two commercial SBSs [Solprene 416 (P1) and Solprene 411 (P2)] and their corresponding partially hydrogenated SBEBSs. In particular, this work explores the effect of the concentration and characteristics of the polymer on the morphology and rheological behavior of maltene–polymer mixtures.

EXPERIMENTAL

Materials

Materials used for the hydrogenation of SBS and polymer characterization. Were ultrahigh-purity hydrogen (99.99%) and ultrahigh-purity nitrogen (Praxair, México D.F., México), cyclohexane (Dynasol, Tamaulipas, México), nickel (II) bisacetylacetonate, n-butyllithium [Lithium Division, FMC; 16% (w/w) in cyclohexane, Bessenmer, North Carolina, USA], tert-butylhydroxytoluene (BHT; Sigma Aldrich, Edo. México, México), and tetrahydrofuran (THF; J.T. Baker, México D.F., México).

Maltenes

The maltenes used in this work were obtained by the subjection of Ac-20 asphalt (Pemex, Salamanca, Mexico) to the *n*-heptane selective solubilization process (ASTM D 3279-90 and ASTM D 4124-86). Industrial *n*-heptane was used as received.

Polymers

Four different polymers were used: two commercial polymers (P1 and P2; Dynasol) and two other polymers produced by the catalytic hydrogenation of the commercial polymers. The two commercial polymers had a four-branch, starlike chain architecture, with polybutadiene midblocks and polystyrene end blocks (i.e., SBS type) and the same overall composition but different average molecular weights Polystyrene (wt %) changes to Styrene (wt %) and Saturated vinyl (%) by NMR changes to 1,2-Vinyl saturation (%) by NMR (Table I). The two partially hydrogenated polymers (P1H and P2H) were prepared by homogeneous hydrogenation of P1 and P2, respectively, with a catalyst based on nickel(II) bisacetylacetonate and *n*-butyllithium. Through the control of the hydrogenation degree of P1 and P2, two SBEBS-type polymers were produced, both having a starlike chain architecture with poly[(butadiene)$_{1-x}$–(ethylene-*co*-butylene)$_x$] midblocks and polystyrene end blocks of the same size as those of their parent SBS.

TABLE I
Properties of the Polymers Used To Prepare the MPBs: SBS and SBEBS

Polymer	Monomer distribution	Polystyrene (wt %)	$M_{n,\text{total}}$ (g/mol)	Polydispersity index (M_w/M_n)	1,2-Vinyl (%) by NMR	Saturated vinyl (%) by NMR	Global saturation (%) by NMR	$T_{g,\text{PB}}$ (°C)	T_m (°C)	Crystallinity (%) by DSC
SBS1 (P1)	Block	30	149,000	1.06	7.71	0	0	−92	—	Amorphous
SBS2 (P2)	Block	30	265,000	1.03	7.69	0	0	−92	—	Amorphous
SBEBS1 (P1H)	Block	30	153,000	1.07	0	100	60.48	—	54	7
SBEBS2 (P2H)	Block	30	267,000	1.09	0	100	49.55	—	59	1

M_n = number-average molecular weight; $M_{n,\text{total}}$ = total number-average molecular weight; M_w = weight-average molecular weight; $T_{g,\text{PB}}$ = polybutadiene glass-transition temperature; T_m = melting temperature. SEC, size exclusion chromatography. NMR, nuclear magnetic resonance. DSC, differential scanning calorimetry.

Blends

Maltene–polymer blends (MPBs) were produced by a high-temperature batch mixing process with well-known amounts of maltenes and SBS or SBEBS.

Methods

Asphalt-selective solubilization process

Maltenes were obtained according to standard methods for maltene–asphaltene separation: ASTM D 3279-90 and ASTM D 4124-86. Known amounts of asphalt and *n*-heptane [ca. 10% (w/w)] were mixed and subjected to an atmospheric (586 mmHg) refluxing process at 90°C for 3 h and were then cooled to room temperature. The *n*-heptane-immiscible asphaltenes were filtered with glass wool, and the maltene *n*-heptane solution was subjected to a distillation process (98°C) to recover the maltenes. Finally, the maltenes were dried at 100°C *in vacuo* (−240 mmHg), and this resulted in a brown, viscous liquid at room temperature.

Hydrogenation

SBS–cyclohexane solutions [ca. 10% (w/w)] were homogeneously hydrogenated[29] with a Ziegler–Natta-type catalyst with a Ni/Li molar ratio of 1/3. The catalyst was prepared as follows: nickel(II) bisacetylacetonate was weighed under a nitrogen atmosphere (2.5 mmol of nickel/100 g of polymer) and then mixed with 50 mL of previously purified THF; then, *n*-butyllithium was slowly added with stirring to prevent the formation of insoluble agglomerates. At the beginning, the solution exhibited a light green color, and as the cocatalyst was added, the solution progressively changed to a dark brown color. Hydrogenation was carried out in a 1-L glass-jacketed reactor equipped with a glass jacket and an internal stainless steel coil for heat exchange. To prevent catalyst deactivation, the number of *n*-butyllithium scavenger substances (mainly humidity and polymer antioxidants) was minimized with the following procedure:[30]

1. The reactor was twice purged with ultrahigh-purity nitrogen to lower the in-gas initiator deactivating substances and to maintain an inert atmosphere.
2. The desired amount of the solvent was then fed to the reactor and treated with *n*-butyllithium, according to a colorimetric titration process, to minimize residues of initiator scavengers.
3. The desired amount of SBS was fed into the reactor, and the temperature was increased up to 50°C with slow stirring; such conditions were maintained until SBS was totally dissolved (ca. 5 h).
4. The SBS–cyclohexane solution was heated up to the hydrogenation temperature (60°C), and the titration procedure was then applied again to eliminate the initiator scavengers. Then, a known amount of the catalyst was added, and subsequently, hydrogen was fed into the reactor; a pressure of 40 psi was maintained during the entire hydrogenation process.

To interrupt the hydrogenation process at the desired level, the catalyst was deactivated with a hydrochloric acid solution [1% (w/v)]; then, a BHT cyclohexane solution (0.8 g of BHT/100 mL of cyclohexane) was mixed with the polymer solution to prevent thermal degradation of the polymer. Samples of the polymer solution were treated with methanol to precipitate the hydrogenated polymer, which was finally dried (50°C) in a vacuum oven overnight.

Blending

Blends of maltenes with 3 or 10% (w/w) SBS or SBEBS were prepared by a simple hot-mixing process with a stainless steel tank equipped with a jacket and stirrer (Yellow Line OST 20, IKA, Staufen, Germany); a nitrogen atmosphere blanket was used to minimize polymer degradation. A predetermined amount of maltenes (ca. 40 g) was fed into the tank and heated up to 60°C with stirring; then, the desired amount of a previously prepared polymer–cyclohexane solution (0.1 g/mL) was gradually added under continuous stirring (500 rpm, 15–20 min), after which the temperature was increased up to 160°C, and this condition was maintained for 3 h to ensure that the MPBs reached pseudo-equilibrium conditions.

Characterization

The average molecular weights and polydispersities of the polymers were determined by SEC with an HP1090 high-performance liquid chromatograph equipped with a PLgel column (5 μm) for 600–10^6 g/mol; THF solutions of polymers and polystyrene standards (ca. 2.4 mg/mL) were analyzed at a constant temperature (40°C). ^{1}H-NMR spectra were obtained with a Varian Unity Inova 300-MHz spectrometer (California, USA) at room temperature with $CDCl_3$ as the solvent and tetramethylsilane as the internal standard. The SBS degree of hydrogenation was determined by a comparison of the ^{1}H-NMR spectrum of the hydrogenated sample SBEBS with that of its parent SBS; the peak areas of the olefinic proton signals at 4.6 (1,2-vinyl) and 5.8 ppm (1,4-cis and 1,4-trans) were used.[31,32] Differential scanning calorimetry (DSC) measurements were carried out

on a Mettler-Toledo 2000 differential scanning calorimeter (México D.F., México). Thermograms covering the range of −130 to 130°C were recorded at a heating rate of 10°C/min; results from the second cycle are reported. The morphology of the blends (i.e., distribution and shape of the polymer-rich phase) was observed in images from fluorescence microscopy analysis of the blends with a Carl-Zeiss KS 300 (New York, USA) microscope equipped with a lamp for wavelengths of 390–459 nm and a 20× lens. The rheological behavior of maltenes and maltene–polymer samples was examined with an AR-2000 strain-controlled rheometer from TA Instruments (New Castle, USA) using parallel-plate geometry (25-mm diameter and 0.5-mm gap). The storage or elastic modulus (G') and loss or viscous modulus (G'') were determined through small-amplitude oscillatory shear flows at frequencies ranging from 0.1 to 300 rad/s at various temperatures under linear viscoelastic conditions. From strain sweep runs, the upper limit of the linear viscoelastic zone was located at strain of about 0.05. In this domain, the experimental tests were essentially nondestructive and could be interpreted in terms of the molecular structure of the material. All samples were tested at various temperatures (25, 40, 50, 60, 70, and 80°C) at least twice. This information was used to construct master curves of G', G'', G^*, and the phase angle (δ), with which the rheological behavior of the blends was explained.

RESULTS

It is convenient to explain first the nomenclature of the samples: M stands for maltenes, the number following it represents the polymer content as a weight percentage [i.e., 3 or 10% (w/w)], and the last two (or three) characters identify the polymer. For example, M3PH1 represents an MPB with 3% (w/w) polymer PH1, PH1 being an SBEBS obtained by the partial hydrogenation of P1.

Polymer average molecular weights

Figure 1 displays the SEC chromatograms of P2 and P2H; they have similar elution times (similar results were also obtained for P1 and P1H), and this indicates that both nonhydrogenated P2 and corresponding partially hydrogenated P2H have practically the same average molecular weights, as reported previously.[18,32] During the hydrogenation process, the polymer molecular weight increases because of the incorporation of two hydrogen atoms for each saturated double bond; however, chain scission and crosslinking may also occur.[32] Depending on the degree of saturation, the capacity of the hydrogenated polymer for interacting with THF (carrier) can differ from that of the nonhydrogenated polymer. P1 and P2 are amorphous, whereas their partially hydrogenated counterparts, P1H and P2H, exhibit a certain degree of crystallinity, and such a difference may have an effect on the THF–polymer interaction. Then again, the experimental error for SEC analysis of this kind of polymer can be up to 2%, which is close to the difference in the elution times of P2 and P2H. Therefore, on the basis of the information available, the small difference between the elution times of P2 and P2H (Fig. 1) cannot be explained without doubt. Table I shows the average molecular weights of the SBS and SBEBS used in this work. These results confirm that such a hydrogenation process is mild enough to partially saturate a number of double bonds of the SBS poly(butadiene-*block*) without promoting a considerable amount of polymer degradation.

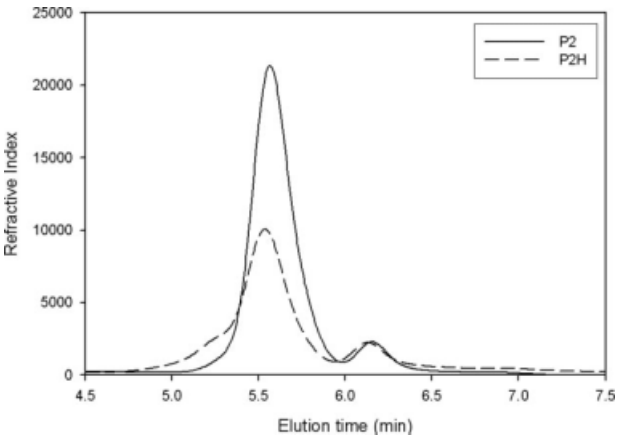

Figure 1 SEC chromatograms of the copolymers (A) P2 and (B) P2H.

SBS hydrogenation

The ^{1}H-NMR spectra of a given SBS and its corresponding SBEBS were used to determine the relative amounts of 1,4-cis, 1,4-trans, and 1,2-vinyl units of the elastomeric block of the SBEBS. The global saturation of polymers PH1 and PH2 was calculated with the equations previously reported.[18,32] As the same characteristic peaks appear for all these samples, the discussion is limited to the spectra of P1 and its hydrogenated analogue P1H. By comparing the spectrum of P1 with that of P1H (Fig. 2), we find that PH1 exhibits a considerable increase in the signals of the aliphatic protons (1.43–2.03 ppm), whereas the signals attributed to the phenyl protons of the styrenic block (6.52–7.07 ppm) remain practically unaltered; this indicates that saturation occurs exclusively on the double bonds of the polybutadiene. Table I shows the global composition and microstructure of the elastomeric block of the SBS and SBEBS reported here.

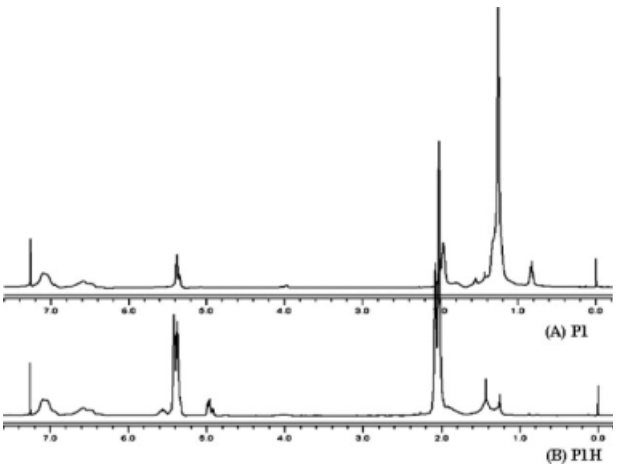

Figure 2 ^{1}H-NMR (300 MHz) spectra of copolymers (A) P1 and (B) P1H.

Thermal properties of the polymers

Thermograms of polymers P1 and P1H are shown in Figure 3, from which the glass-transition temperature (T_g) of P1 and crystallinity percentage of PH1 were estimated; the same procedure was used for analyzing P2 and P2H. Table I shows the results of the thermal analysis.

Thermograms of the neat samples of P1 and P2 show that these polymers exhibit only the T_g corresponding to the polybutadiene block; these results, combined with the absence of both the T_g of the polystyrene block and a fusion peak, indicate that both samples are composed of a relatively large polybutadiene block and that they are amorphous. In contrast, the hydrogenated polymers PH1 and PH2 display only a fusion peak, and this indicates that saturation of the polybutadiene double bonds produces an elastomeric block with a certain degree of crystallinity.

The results from SEC, ^{1}H-NMR, and DSC reveal that the four polymers used in this study differ from each other in terms of the molecular weight, block size, and/or microstructure of the elastomeric middle block, as shown in Table I. Furthermore, because all MPBs were prepared and analyzed under similar conditions, we expected the morphology and rheological behavior of the blends to be in some way related to the characteristics of these polymers.

Morphology

In Figure 4 are shown representative examples of fluorescence microscopy images of MPBs.

In all cases, two distinct phases are clearly identified: the light field corresponds to the polymer-rich phase, and the dark regions identify the maltene-rich phase. Clearly, regardless of the type (SBS or SBEBS) and concentration of the polymer [3 or 10% (w/w)], all MPBs are biphasic heterogeneous systems. The heterogeneity of these blends, along with the fact that they all exhibit a polymer-rich network with relatively small and spherical maltene inclusions, also reveals a certain degree of incompatibility between some components of the maltenes (i.e., aliphatic and resins) and the polymers in question, as reported for SEBS-modified asphalts.[16,27] According to these results, within the investigated range of compositions, neither the molecular weight [(Fig. 4(C) vs 4(D) and Fig. 4(E) vs 4(F)] nor the type of polymer [Fig. 4(C) vs 4(E) and Fig. 4(D) vs 4(F)] have a significant effect in determining the morphology of the MPBs. These results are explained by the fact that the compatibility which exists between the maltenes and these polymers determines the characteristics of the blend's polymer-rich phase. All four polymers (P1, PH1, P2, and PH2) have a triblock starlike architecture and differ from each other in terms of their molecular weight and/or the composition of the elastomeric middle block: polybutadiene for SBS and poly[(butadiene)$_{1-x}$–(ethylene-*co*-butylene)$_x$] for SBEBS. Therefore, it is thought that these MPBs may have a three-dimensional thermoplastic network composed of nodules of polystyrene blocks interconnected through maltene-swollen elastomeric blocks, which occupy a considerably larger volume than those of the neat polymers (SBS and SBEBS).[9,19,21] On the other hand, the solubility parameters of the maltenes (17.4–26.6 MPa$^{1/2}$) are closer to that of polybutadiene (16.5–17.6 MPa$^{1/2}$) than to that of poly[(butadiene)$_{1-x}$–(ethylene-*co*-butylene)$_x$] (15.9–16.5 MPa$^{1/2}$);[16] thus, maltenes should be more compatible with SBS than with SBEBS, and consequently, the dispersion of SBS within the maltene matrix should be superior to that of SBEBS. Therefore, the amounts and characteristics of these polymers and particularly the compositions of their elastomeric middle block may have played an

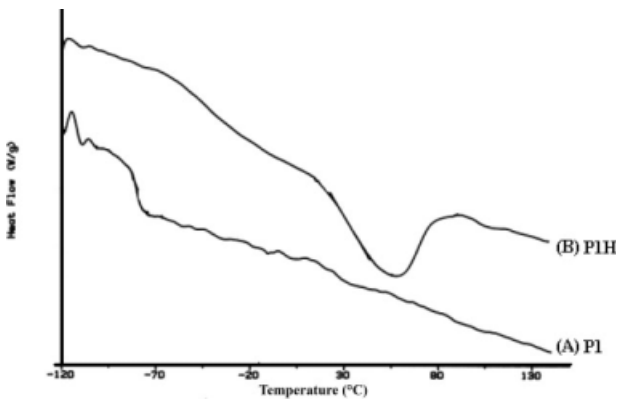

Figure 3 DSC thermograms for copolymers (A) P1 and (B) P1H.

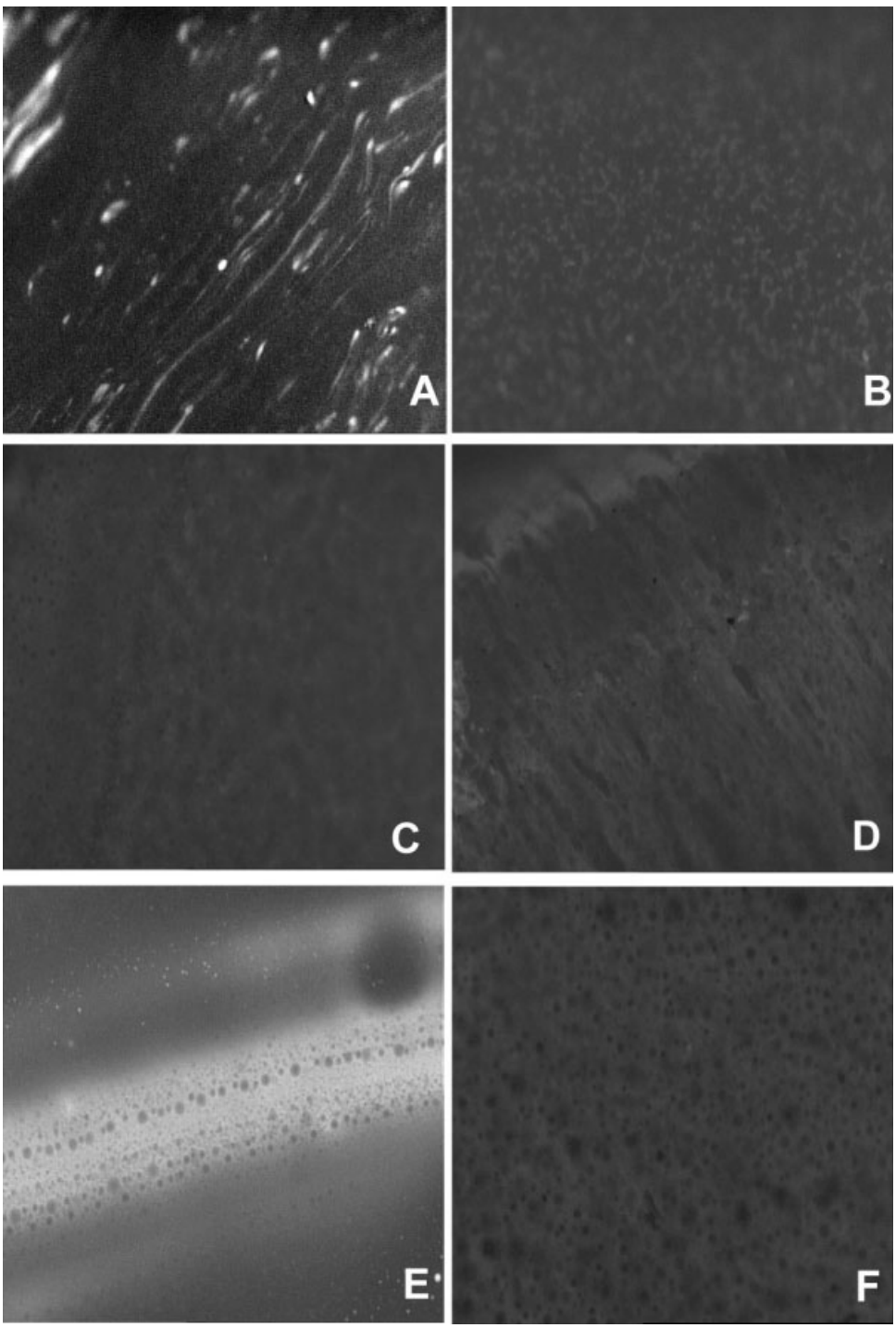

Figure 4 Fluorescence microscopy images (20×) of blends: (A) M3P1, (B) M3P1H, (C) M10P1, (D) M10P2, (E) M10P1H, and (F) M10P2H.

important role in determining the swelling and, consequently, distribution of SBS and SBEBS within the maltenes. However, for the investigated range of compositions, neither the molecular weight nor the composition of the elastomeric middle block of these polymers has a definitive effect on the morphology of the MPBs. It is also important to point out that the morphology observed on the surface of the MPBs does not provide information concerning the bulk structure of the blends, which is most likely to affect the mechanical behavior of the MPBs.

Rheology

The rheological characterization of neat maltenes (NMs) and MPBs provided information about the

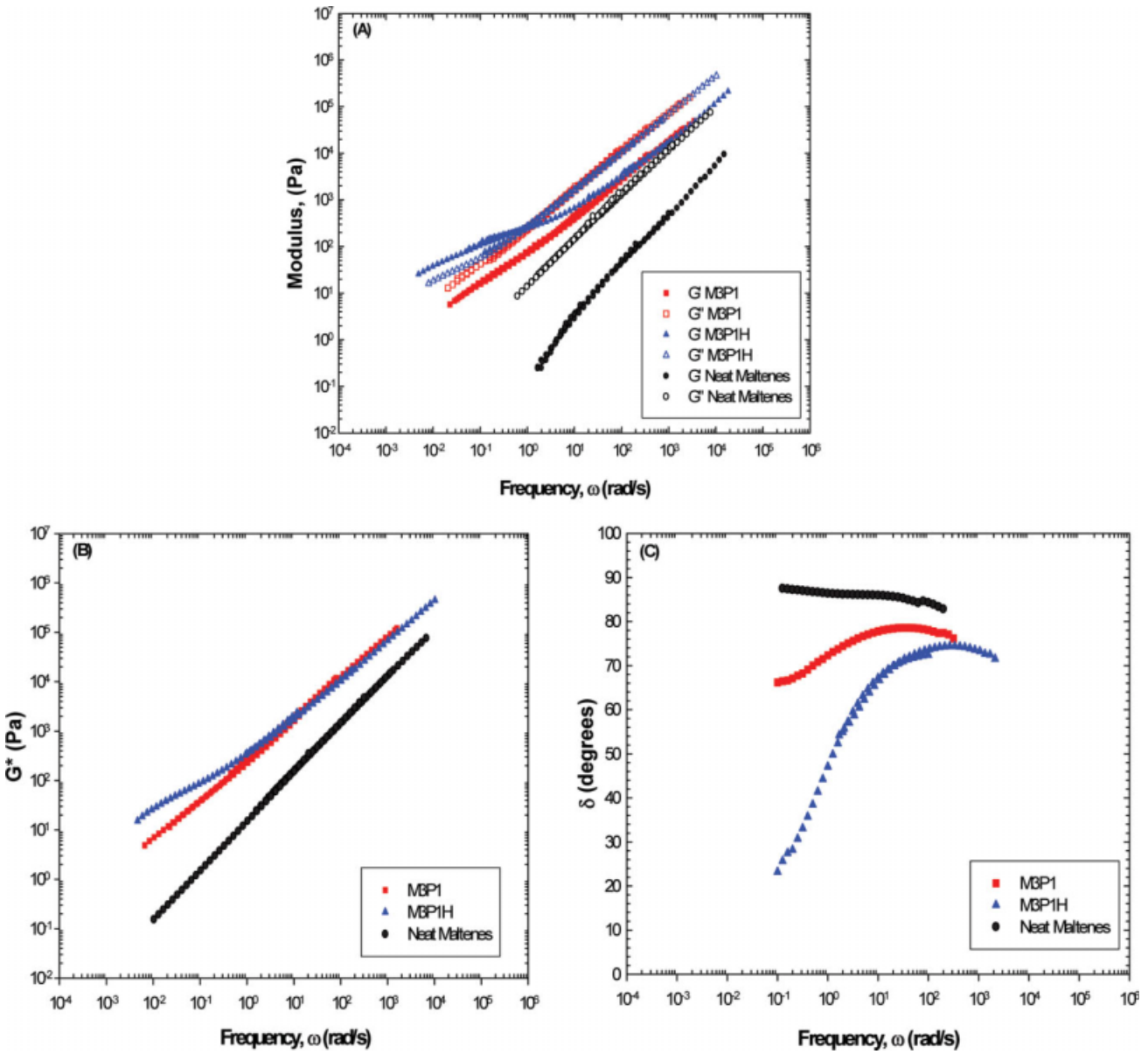

Figure 5 (A) Master curves of G'' and G' for NMs, M3P1, and M3P1H (reference temperature = 50°C); (B) master curves of G^* for NMs, M3P1, and M3P1H; and (C) master curves of δ for NMs, M3P1, and M3P1H. [Color figure can be viewed in the online issue, which is available at www.interscience.wiley.com.]

resistance to deformation of these materials when subjected to shear loading. The results of such experiments are presented as master curves of G', G'', G^*, and δ, which were created by the application of the time–temperature superposition principle[17,26,33] with 50°C as the reference temperature. G' and G'' are material functions that represent the molecular structure of the material; G^* represents the viscoelastic nature of the material, combining its viscous and elastic responses ($G^* = G' + iG''$); and δ is a measure of the viscoelastic balance of the material behavior ($\tan \delta = G''/G'$) and is considered more sensitive to the structure of the sample than G^*.[9,17] To examine how the rheological behavior of the MPBs is affected by the properties of the polymer, such as the molecular weight and composition of the elastomeric block, the rheological data of MPBs are presented as well as those of NM as a reference. The results have been organized as follows: Figures 5 and 6 show the results of low-polymer blends [3% (w/w)], whereas Figures 7 and 8 show the data for high-polymer blends [10% (w/w)].

The rheological behavior of MPBs, regardless of the type of polymer used in their preparation, differs from that of NM, as shown in the master curves from a high shear frequency to a low shear frequency (i.e., increasing temperature). All blends exhibit higher G' and G'' values, which when

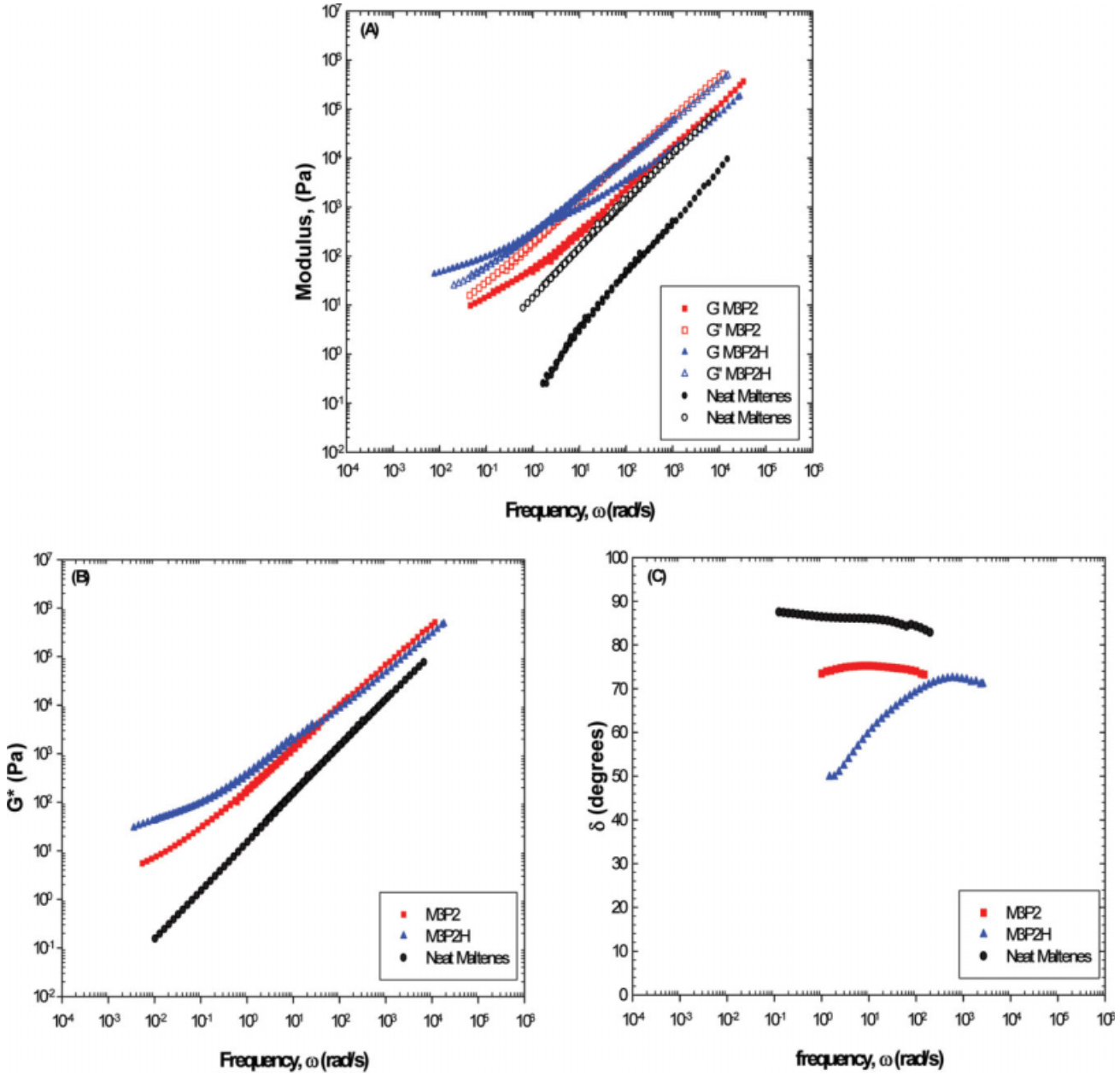

Figure 6 (A) Master curves of G'' and G' for NMs, M3P2, and M3P2H (reference temperature = 50°C); (B) master curves of G^* for NMs, M3P2, and M3P2H (reference temperature = 50°C); and (C) master curves of δ for NMs, M3P2, and M3P2H (reference temperature = 50°C). [Color figure can be viewed in the online issue, which is available at www.interscience.wiley.com.]

combined result in higher viscoelasticity and elastic character. Nonetheless, the rheological behavior of MPBs is influenced by both the characteristics of the polymer and its composition in the blend.

Low-polymer blends

The results of the rheological characterization of blends with a low polymer content [i.e., 3% (w/w)] are shown in Figures 5 and 6.

The analysis of the data presented in Figures 5 and 6 was performed by the arbitrary division of the entire frequency range into regions of high frequency ($\omega > 10^1$ rad/s) and low frequency ($\omega < 10^1$ rad/s). Figure 5(A) presents master curves of $G'(\omega)$ and $G''(\omega)$ for NM, M3P1, and M3PH1. NM shows viscous behavior ($G' < G''$) within the frequency range examined (10^{-2} rad/s $< \omega < 10^5$ rad/s), with a reduction of both the viscoelasticity [Fig. 5(B)] and elastic character [Fig. 5(C)] as the frequency decreases, eventually displaying completely viscous behavior ($\delta \approx 90°$) at $\omega \approx 10$ rad/s. These results suggest that, within the range of frequencies investigated, NM behaves as a viscoelastic material able to

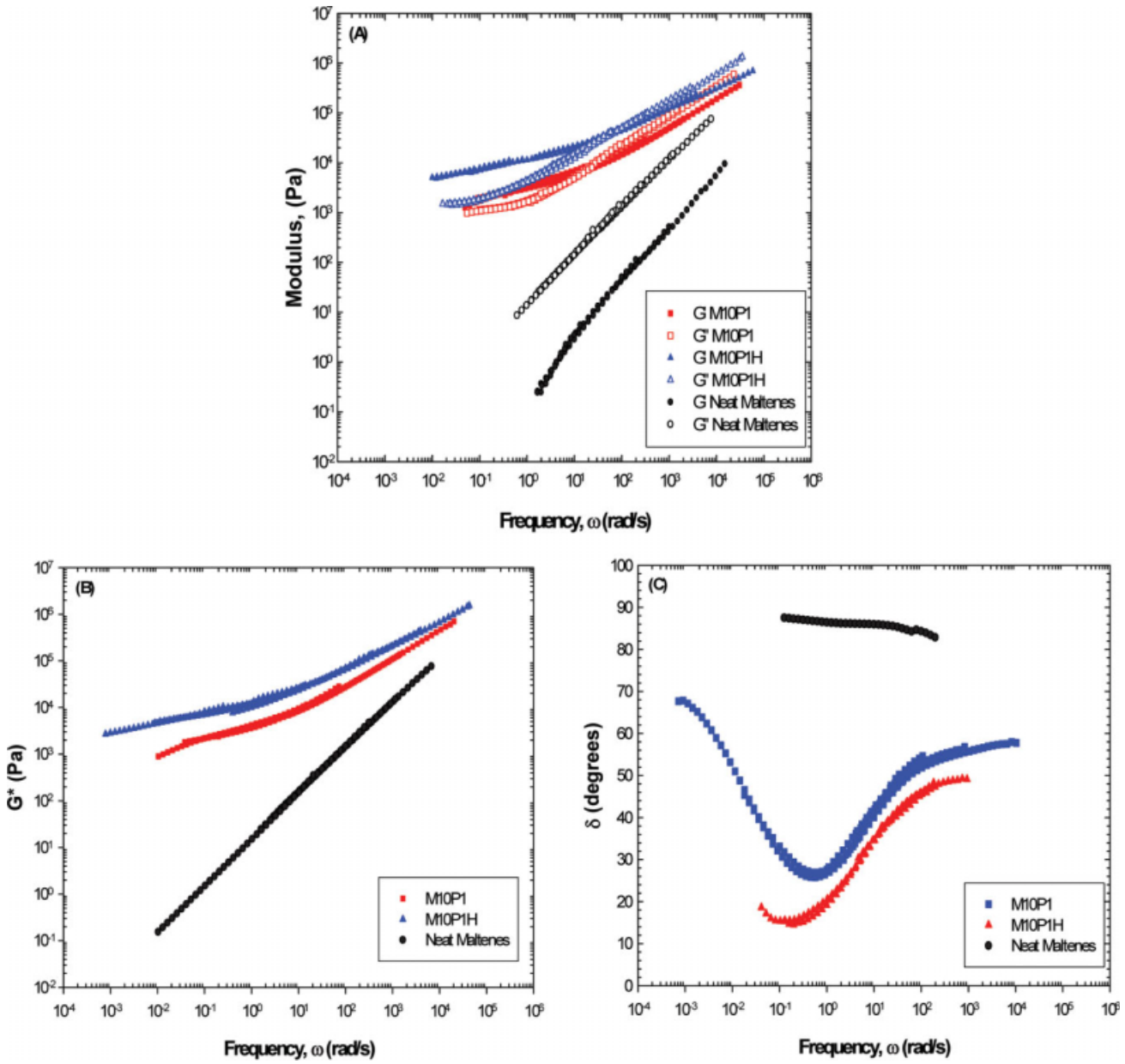

Figure 7 (A) Master curves of G'' and G' for NMs, M10P1, and M10P1H (reference temperature = 50°C); (B) master curves of G^* for NMs, M10P1, and M10P1H (reference temperature = 50°C); and (C) master curves of δ for NMs, M10P1, and M10P1H (reference temperature = 50°C). [Color figure can be viewed in the online issue, which is available at www.interscience.wiley.com.]

dissipate stress without presenting structural changes. In contrast, M3P1 exhibits a higher elastic character, responding to decreasing shear frequency with viscous behavior ($G' < G''$), decreasing viscoelasticity [$-dG^*/d\omega \approx 10$; Figure 5(B)], and increasing elasticity [from $\delta \approx 80^\circ$ for $\omega > 10^0$ rad/s up to $\delta \approx 65^\circ$ at $\omega \approx 10^{-1}$ rad/s; Fig. 5(C)]. Figure 5(A) also shows that the rheological behavior of M3PH1 is considerably different from that of M3P1 because as the frequency decreases, G' of M3PH1 increases more than G'', reaching a crossover frequency (ω_c) at 228 Pa ($G' = G'' \approx 228$ Pa at $\omega_c \approx 1$ rad/s), at which point it behaves as an elastic material ($G' > G''$). Figure 5(B) shows that M3P1 and M3PH1 have comparable viscoelastic profiles at a high frequency ($-dG^*/d\omega \approx 6.7$ for $\omega > 10^0$ rad/s); however, at lower frequencies, M3PH1 displays increasing viscoelasticity ($-dG^*/d\omega \approx 4.8$ for $\omega < 10^0$ rad/s). In addition, Figure 5(C) clearly shows that at a high frequency, M3P1 and M3PH1 exhibit a more or less constant elastic character ($\delta < 80^\circ$ for $\omega < 10^2$ rad/s); then, as the frequency decreases, the elastic

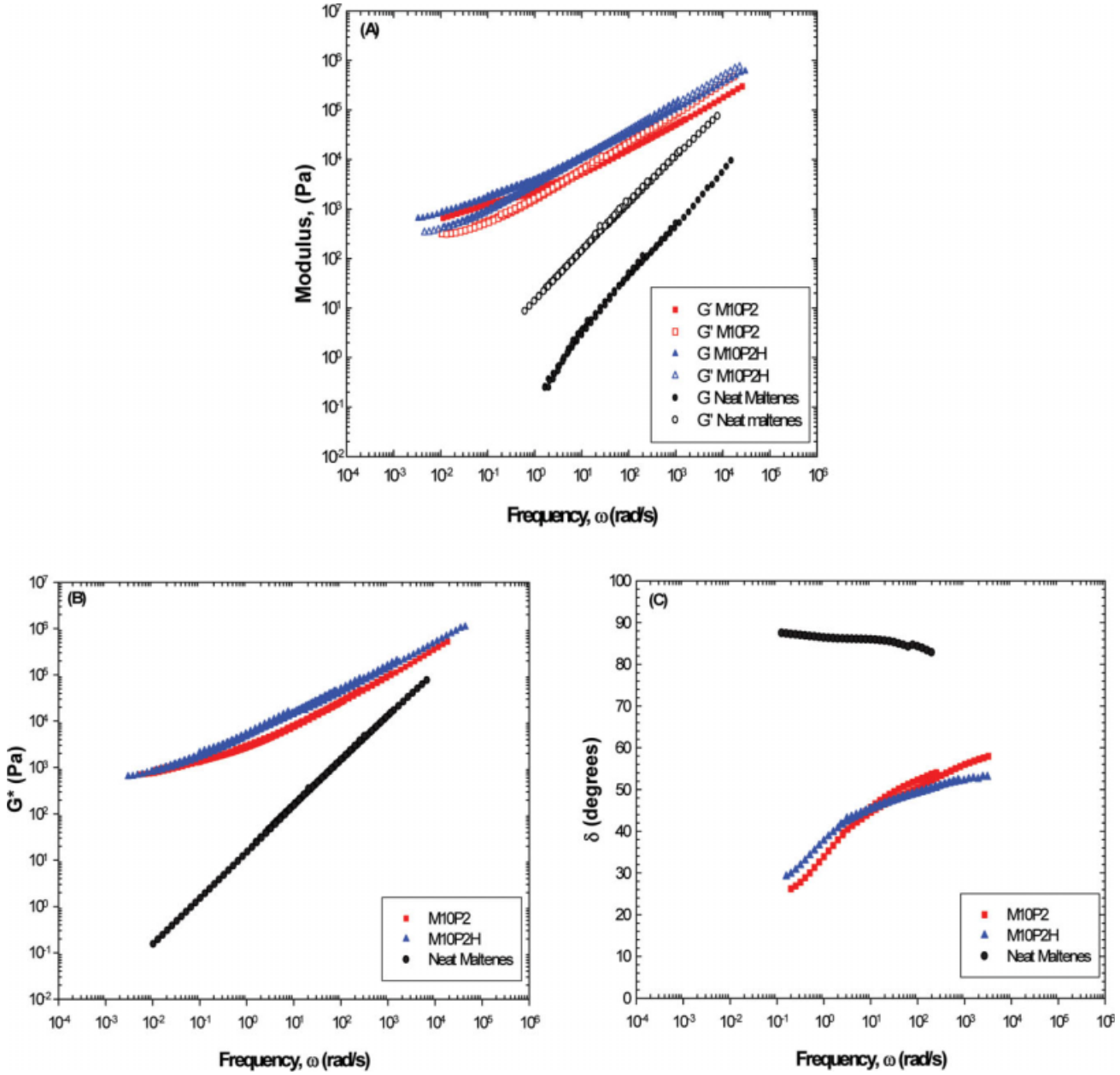

Figure 8 (A) Master curves of G'' and G' for NMs, M10P2, and M10P2H (reference temperature = 50°C); (B) master curves of G^* for NMs, M10P2, and M10P2H (reference temperature = 50°C); and (C) master curves of δ for NMs, M10P2, and M10P2H (reference temperature = 50°C). [Color figure can be viewed in the online issue, which is available at www.interscience.wiley.com.]

character of M3PH1 considerably changes (from 80 to 25°) in comparison with that of M3P1 (from 80 to 76°).

Figure 6 presents the master curves of M3P2 and M3P2H. It is clear from a comparison of Figures 5 and 6 that the rheological behavior displayed by M3P2 and M3P2H is similar to that of M3P1 and M3P1H, respectively. M3P1 and M3P2 exhibit rather similar rheological behavior within the entire range of frequencies investigated ($10^{-2} < \omega < 10^4$ rad/s), exhibiting similar viscoelasticity and elastic character. Moreover, when these results are compared with those of the maltenes, it is clear that even small amounts of polymers P1 and P2 [3% (w/w)] affect the magnitude of both G'' and G' [Figs. 5(A) and 6(A)] as well as the viscoelasticity [Figs. 5(B) and 6(B)] and elastic character [Figs. 5(C) and 6(C)] of the maltenes, particularly at a low frequency ($\omega < 2 \times 10^0$ rad/s). These results suggest that the SBS copolymers have been well incorporated within the maltenes, and consequently, the polymer-rich phase is determining the rheological behavior of the blend. On the other hand, M3PH1 and M3PH2 exhibit similar rheological behavior, displaying similar $G'(\omega)$

and $G''(\omega)$ profiles with practically the same crossover frequency ($\omega_c = 1$ rad/s). However, at a high frequency ($\omega > 10^1$ rad/s), M3PH2 exhibits higher viscoelasticity. In terms of $\delta(\omega)$, both M3PH1 and M3PH2 present a plateau of $\delta \approx 70^\circ$ within the frequency range of $5 \times 10^1 < \omega < 2.5 \times 10^3$ rad/s, although at lower frequencies M3PH2 displays higher elastic character ($\delta \approx 48^\circ$).

These results led to the conclusion that the microstructure of the elastomeric block of SBS and SBEBS plays an important role in determining the rheological behavior of their maltenes blends. Because the solubility parameter of maltenes is more similar to that of SBS than it is to that of SBEBS,[16,22] it is possible that the polymer-rich phase of MPBs prepared with SBS is different from that of MPBs prepared with SBEBS, resulting in different rheological behavior. Regarding the effect of the molecular weight, these results demonstrate that at such a low polymer concentration [i.e., 3% (w/w)], the difference between the molecular weights of P1 and P2 (149,000 and 265,000 g/g mol, respectively; Table I) does not strongly affect the rheological behavior of their blends (M3P1 and M3P2, respectively). The same conclusion can be reached for blends prepared with PH1 and PH2 (M3PH1 and M3PH2, respectively). Along with the effect of molecular weight, these two polymers differ from each other in terms of the composition of the elastomeric middle block (refer to Table I).

High-polymer blends

Data from the rheological characterization of blends with a high polymer content [i.e., 10% (w/w)] are shown in Figures 7 and 8.

Again, the analysis of the data presented in Figures 7 and 8 considers two arbitrarily defined frequency regions: high ($\omega > 10^1$ rad/s) and low ($\omega < 10^1$ rad/s). Figure 7 presents data for MPBs prepared with high-molecular-weight polymers (265,000 g/g mol), both neat (M10P1) and partially hydrogenated (M10P1H). The data shown in Figure 8 correspond to MPBs prepared with low-molecular-weight polymers (149,000 g/g mol), also both nonhydrogenated (M10P2) and partially hydrogenated (M10P2H).

As revealed in Figure 7(A), M10P1 displays viscous behavior at a low frequency with a crossover ($G' = G'' = 8 \times 10^3$ at $\omega \approx 2 \times 10^1$ rad/s) and elastic behavior ($G' > G$) at a higher frequency. Although similar trends were observed for M10P1H, its G' and G'' values and crossover frequency ($G' = G'' = 3 \times 10^4$ at $\omega \approx 8 \times 10^1$ rad/s) are higher than those of M10P1. Figure 7(B) shows the viscoelasticity of M10P1 and M10P1H in terms of their master curves of $G^*(\omega)$. It is evident that G^* of both blends decreases as the frequency decreases; however, M10P1H is more viscoelastic, and the rate of change of its viscoelasticity is lower that that of M10P1 at both high and low frequencies. With respect to the elastic character of M10P1 and M10P1H, Figure 7(C) shows that these two blends have a complex $\delta(\omega)$ profile, exhibiting various slope changes, M10P1H being the more elastic. At a high frequency ($\omega > 10^2$ rad/s), both display a more or less constant and different elastic character (M10P1H, $\delta = 58^\circ$, and M10P1, $\delta = 50^\circ$). As the frequency decreases, the elasticity of both blends increases at about the same rate of change until a minimum is reached (M10P1H, $\delta = 14^\circ$ at $\omega = 2 \times 10^{-1}$, and M10P1, $\delta = 26^\circ$ at $\omega = 5 \times 10^{-1}$); from there, the elasticity of these two blends deceases with a similar rate of change.

Figure 8 shows the rheological behavior of M10P2 and M10P2H. Comparing the results of M10P2 and M10P2H (Fig. 8) with those of M10P1 and M10P1H (Fig. 7), we find that the effects of the molecular weight and the composition of the elastomeric middle block on the rheological behavior of the high-polymer MPBs are established. Contrasting data shown in Figures 7(A) and 8(A) have led to the following observations. First, like M10P1, M10P2 displays viscous behavior at a low frequency and elastic behavior at a higher frequency; however, M10P2 shows a crossover at a lower frequency than M10P1 ($G' = G'' = 1 \times 10^3$ at $\omega \approx 5 \times 10^0$ rad/s vs $G' = G'' = 9 \times 10^3$ at $\omega \approx 2 \times 10^1$ rad/s). Second, compared with M10P1H, M10P2H has lower values of G' and G'', and its $G'(\omega)$ and $G''(\omega)$ profiles overlap for a considerable range (10^0 rad/s $< \omega < 10^2$ rad/s), whereas M10P1H exhibits a distinct crossover (8×10^1 rad/s). Figure 8(B) shows that at a low frequency ($\omega \approx 3 \times 10^{-2}$ rad/s), M10P2 is less viscoelastic than M10P2H; after this point, their viscoelasticity is similar. Figures 7(B) and 8(B) also show that (1) M10P1 is slightly more viscoelastic than M10P2, (2) MPBs prepared with SBS (i.e., M10P1 and M10P2) exhibit lower viscoelasticity than those prepared with the corresponding SBEBS (i.e., M10PH1, and M10PH2, respectively), and (3) M10PH1 is clearly more viscoelastic than M10PH2. Comparing the δ data for high-polymer MPBs [Figs. 7(C) and 8(C)], we can make the following observations: (1) for $\omega > 3 \times 10^1$ rad/s, M10P1 and M10P2 exhibit similar elastic character, whereas for 10^0 rad/s $< \omega < 2 \times 10^1$ rad/s, M10P1 is more elastic; (2) M10P1 exhibits less elastic character than M10PH1; (3) for $\omega < 10^1$ rad/s, M10P2 is more elastic than M10PH2, but it is less elastic for $\omega > 10^1$ rad/s; and (4) the $\delta(\omega)$ profiles of M10P2 and M10P2H are less complex than those of M10P1 and M10P1H.

In summary, both low- and high-polymer blends display higher viscoelasticity and elastic character than NM, and such differences are more evident

when the samples are subjected to a low shear frequency. Also, MPBs prepared with SBEBS are more viscoelastic and have more complex elastic profiles than those based on SBS, so the elastomeric middle block of SBS and SBEBS has a definite effect on the rheological behavior of their MPBs. In contrast, the polymer molecular weight has a negligible effect on the rheological behavior of blends with the same elastomeric block composition of the polymer. Furthermore, by comparing the results of low-polymer blends (Figs. 5 and 6) with those of high-polymer blends (Figs. 7 and 8), we find that the increase in the polymer concentration extends both the viscoelastic and elastic character of the MPBs, and this effect is more significant for SBEBS-based MPBs.

To explain these results, it is worth recalling that the MPBs were prepared by a hot-mixing process with the same lot of maltenes and four different polymers (P1, P2, P1H, and P2H). All these polymers have a starlike architecture with four equal arms (elastomer-*b*-polystyrene) radiating outward with an elastomeric core. These polymers have the same styrene content [30% (w/w)] but differ in the molecular weight (P1 and P1H, 149,000 g/g mol, and P2 and P2H, 265,000 g/g mol) and in the composition of the elastomeric midblock. Because of their molecular architecture and composition, these polymers develop tridimensional networks, with the elastomeric midblocks being the threads and the polystyrene end blocks being the nodes. It is also convenient to emphasize that all blends were prepared by the same hot-mixing process, during which the maltenes and polymer were brought into intimate contact, and because of the similarity or disparity of the solubility parameters between the maltenes and SBS or SBEBS, the elastomeric part of the polymer was swollen with maltenes; this increased the volumetric contribution of the polymer to the blends. It has been reported[16,22] that maltenes are more compatible with SBS than with SBEBS, and such a difference should have an impact on the characteristics of the polymer-rich phase and hence the rheological behavior of the blends prepared with these polymers. On the basis of the results and considerations previously outlined, it is assumed that all the MPBs examined are heterogeneous materials composed of a polymer-rich phase and a maltene-rich phase. The polymer-rich phase is presumed to form a three-dimensional network, with threads of maltene-swollen elastomeric midblocks tied through polystyrene end blocks. The maltene-rich phase is composed of maltenes that did not participate in swelling of the polymer. Because the attributes of the polymer-rich phase are determined by the compatibility between the maltenes and polymer, it is thought that both the amounts and molecular characteristics of the SBS and SBEBS, such as the molecular weight and composition of their elastomeric block, play important roles in determining the characteristics of MPBs. Depending on the polymer content of the MPB, the polymer-rich phase is either the disperse phase or the continuous phase. Results of the analysis of the MPBs by fluorescence microscopy indicate that both low- and high-polymer blends exhibit considerable swelling of the polymer by maltenes, regardless of the degree of hydrogenation. Therefore, this technique provides limited information on the effect of the extent of hydrogenation on MPB morphology. Rheological characterization, on the other hand, provides more information of the MPBs: (1) in contrast to the rheological behavior of NMs, all polymer blends are biphasic viscoelastic materials that dissipate stress by undergoing structural changes; (2) the increase in the elastic behavior of MPBs can be attributed to the elastic nature of the polymer-rich phase because the viscosity of the maltenes is considerably lower than that exhibited by the MPBs; and (3) the composition of the elastomeric blocks of the investigated SBS or SBEBS plays an important role in determining the rheological behavior of their MPBs.

The rheological behavior of both low-polymer [3% (w/w)] and high-polymer [10% (w/w)] blends can be explained if we consider that the response of the blend is mainly determined by the behavior of the polymer-rich phase.

Composition of the elastomeric block

Blends having SBEBS exhibit higher elasticity than those prepared with SBS because the elastomeric block of the SBEBS is more rigid and less compatible with the maltenes than the polybutadiene block of SBS. Therefore, at lower frequencies, the blends are sensitive to the characteristics of their polymer-rich phase (i.e., chemical structure),[33,34] and their increasing elasticity shows the tendency of the polymer-rich phase to form an elastic network[9,17,26] whose characteristics depend on the blend composition. The δ plateau displayed by all blends is an indication of the presence of a polymer-rich elastic phase with enough entanglements to determine the behavior of the blend. These results confirm the importance of the composition of the elastomeric block of the copolymer in determining the rheological behavior of blends.

Molecular weight

Taking into account that all these polymers are able to develop tridimensional polymer-rich structures, that all these samples were prepared with the same mass of polymer [either 3 or 10% (w/w)] but different amounts of polymer chains, and that the relative

amount of the polymer was enough to form a true polymer-rich network, we find that the rheological behavior of these MPBs is determined by the total number of elastomeric and polystyrene blocks, being independent of the number of polymer chains and thus of the molecular weight of the polymer.

Polymer content

The effect of increasing the polymer content on the rheological properties of the MPBs is to increase the viscoelasticity and complexity of the elastic character of the MPBs. These results are expected because the rheological behavior of the blends is completely determined by the continuous polymer-rich phase. Such an effect is significant on MPBs prepared with SBEBS because these copolymers are less compatible with the maltenes and have a certain degree of crystallinity that make them more rigid than SBS.

CONCLUSIONS

This work reports the effects of the molecular weight, elastomeric block composition, and polymer concentration on the morphology and rheological behavior of MPBs prepared with two types of polymers: SBS and SBEBS. Results of the characterization of neat and partially hydrogenated SBS by SEC, Fourier transform infrared spectroscopy, and ^{1}H-NMR spectroscopy suggest that hydrogenation conditions are adequate to favor saturation of the polybutadiene-block isomers over other reactions such as chain scission, crosslinking, or saturation of the polystyrene block. Consequently, the polymers used in this work have similar overall compositions [30% (w/w) styrene] and differ from one another in the size of the polystyrene blocks and the size and composition of their elastomeric blocks.

Fluorescence microscopy results indicate that all MPBs are biphase heterogeneous systems with polymer-rich and maltene-rich phases, suggesting that these two phases are compatible to a certain extent. The polymer-rich phase can be a three-dimensional network, with threads of maltene-swollen elastomeric midblocks tied through polystyrene end blocks, whereas the maltene-rich phase is composed of maltenes that did not participate in the swelling of the polymer. All MPBs exhibit considerable swelling of the polymer by maltenes, regardless of the composition of the elastomeric midblock. For low-polymer blends, the polymer-rich phase is the disperse phase, and for high-polymer blends, it is the continuous phase. However, this technique provides limited information on how the morphology of the MPBs is affected by the molecular weight and composition of the elastomeric block of the polymer.

The effects of the characteristics of the polymer and polymer concentration on the rheological behavior of MPBs have been investigated by the subjection of samples of NMs and MPBs to small-amplitude oscillatory shear sweeps at various frequencies (0.1–300 rad/s) and temperatures (25, 40, 50, 60, 70, and 80°C), all within a linear viscoelastic zone. Master curves of G', G'', and G^* as well as δ indicate that the maltenes behave as viscoelastic materials that are able to dissipate stress without presenting structural changes, whereas all polymer blends are biphasic viscoelastic materials that seem to dissipate stress by undergoing structural changes. The addition of a polymer to maltenes produces MPBs with higher viscoelasticity and elastic character than those of the NMs, and such an increase is considerably higher in MPBs prepared with SBEBS and with a high polymer content. However, it has been observed that the molecular weight of the polymer does not have an important effect on the rheological behavior of the MPBs with both low and high polymer contents. These results are explained by the fact that all these polymers are able to develop tridimensional polymer-rich structures and the relative amounts of polymer chains are tangled enough to form a true polymer-rich network. Thus, the rheological behavior of these MPBs is determined by the total number of elastomeric and polystyrene blocks, being independent of the number of polymer chains and thus of the molecular weight of the polymer. With respect to the effect of the composition of the elastomeric midblock, rheological characterization has revealed that MPBs prepared with SBEBS are more viscoelastic and have higher elasticity than blends prepared with SBS. Such differences were clearly shown at a lower frequency ($\omega \approx 10^{-1}$ rad/s), at which the nature of the polymer-rich phase determines the rheological behavior of the MPBs. These results prove that the composition of the elastomeric block of SBS and SBEBS has an important effect on the rheological behavior of these blends; and this is explained by the fact that the differences in the compatibility of the maltene–SBS and maltene–SBEBS systems result in different swelling and dispersion behaviors of SBS and SBEBS and thus in MPBs with different viscoelastic characters. As expected, the effect of increasing the polymer content on the rheological properties of the MPBs is to increase the viscoelasticity and complexity of the elastic character of the MPBs because the rheological behavior of the blends is completely determined by the polymer-rich phase. Because SBEBS is less compatible with the maltenes and has a certain degree of crystallinity, the effect of increasing the polymer content is more significant on MPBs prepared with SBEBS than on MPBs prepared with SBS.

This article is a collaboration between Mexico and France.

References

1. Polacco, G.; Biondi, D.; Stastna, J.; Vlachovicova, Z.; Zanzotto, L. Macromol Symp 2004, 218, 333.
2. (a) Corbett, L. W.U.S. Pat. 3,940,281 (1976); (b) Corbett, L. W. Hydrocarbon Process 1979, 58, 173.
3. Stastna, J.; Zanzotto, L.; Vacin, O. J. J Colloid Interface Sci 2003, 259, 200.
4. Champion, L.; Gerard, J. F.; Planche, J. P.; Martin, D.; Anderson, D. J Mater Sci 2001, 36, 451.
5. García-Morales, M.; Partal, P.; Navarro, F. J.; Martínez-Boza, F.; Gallegos, C.; González, N.; Muñoz, M. E. Fuel 2004, 83, 31.
6. Lesueur, D.; Gerard, J. F.; Claudy, P.; Letoffe, J. M.; Planche, J. P.; Martin, D. Rheology 1996, 40, 813.
7. McKay, K. W.; Gros, W. A.; Diehl, C. F. J Appl Polym Sci 1995, 56, 947.
8. González, O.; Muñoz, M. E.; Santamaría, A. Rheol Acta 2006, 45, 603.
9. Airey, G. D. J Mater Sci 2004, 39, 951.
10. Polacco, G.; Stastna, J.; Vlachovicova, Z.; Biondi, D.; Zanzotto, L. Polym Eng Sci 2004, 44, 2185.
11. Isacsson, U.; Lu, X. Mater Struct 1995, 28, 139.
12. García-Morales, M.; Partal, P.; Navarro, F. J.; Martínez-Boza, F. J.; Gallegos, C. Rheol Acta 2006, 45, 513.
13. Fawcett, A. H.; McNally, T. Polymer 2000, 41, 5315.
14. Pérez-Lepe, A.; Martínez-Boza, F. J.; Attané P.; Gallegos, C. J Appl Polym Sci 2006, 100, 260.
15. Lesueur, D.; Gerard, J. F.; Claudy, P.; Letoffe, J. M.; Planche, J. P.; Martin, D. J Rheol 1998, 42, 1059.
16. Polacco, G.; Muscente, A.; Biondi, D.; Santini, S. Eur Polym J 2006, 42, 1113.
17. Becker, Y.; Müller, A. J.; Rodríguez, Y. J Appl Polym Sci 2003, 90, 1772.
18. Vargas, M. A.; Chavez, A. E.; Herrera, R.; Manero, O. Rubber Chem Technol 2005, 78, 620.
19. Wen, G.; Zhang, Y.; Zhang, Y.; Sun, K.; Fan, Y. Polym Test 2002, 21, 295.
20. Wloczysiak, P.; Vidal, A.; Papirer, E.; Gauvin, P. J Appl Polym Sci 1997, 65, 1595.
21. Hsieh, H. L.; Quirk, R. P. Anionic Polymerization—Principles and Practical Applications; Marcel Dekker: New York, 1996.
22. Ho, R. M.; Adedeji, A.; Giles, D. W.; Hajduk, D. A.; Macosko, C. W.; Bates, F. S. J Polym Sci Part B: Polym Phys 1997, 35, 2857.
23. Graeling, D.; Muller, R.; Palierne, J. F. Macromolecules 1993, 26, 320.
24. Hyong-Jun, K.; Yongsok, S. Langmuir 2003, 19, 2696.
25. Carreau, P. J.; Bousmina, M.; Bonniot, F. Can J Chem Eng 2000, 78, 495.
26. Lacroix, C.; Bousmina, M.; Carreau, P. J.; Favis, D. Polymer 1996, 37, 2939.
27. Bousmina, M.; Bataille, P.; Sapieha, S.; Schireiber, H. P. J Rheol 1995, 39, 499
28. Bardet, J. G.; Gorbaty, M. L.; Nahas, N. C.U.S. Pat. 5,248,407 (1993).
29. Hugo, X. S. Master's Thesis, Universidad Nacional Autónoma de México, 2007.
30. Monroy, V.; Guevara, G.; Leon, I.; Correa, A.; Herrera, R. Rubber Chem Technol 1993, 66, 588.
31. Sardelis, K.; Michels, H. J.; Allen, G. Polymer 1984, 25, 1011.
32. Escobar, V. A.; Herrera, R.; Petit, A.; Pla, F. Eur Polym J 2000, 36, 18.
33. Lu, X.; Isacsson, U. Construct Building Mater 1997, 11, 23.
34. Germain, Y.; Ernst B.; Genelot, O.; Dhamani, L. J Rheol 1994, 38, 681.